Pergamon

Int. J. Solids Structures Vol. 31, No. 9, pp. 1225–1240, 1994

0020–7683/94 $6.00 + .00

0020–7683(93)E0030–L

ANALYSIS OF BONDING PROBLEMS UNDER THERMAL LOADING USING THE COMBINED MIXED FUNCTIONAL

DONG SEOK KIM and BYUNG CHAI LEE
Department of Mechanical Engineering, The Korea Advanced Institute of Science and Technology, 373-1 Kuseong-dong, Yuseong-ku, Taejon 305-701, Korea

(*Received* 20 *January* 1993; *in revised form* 13 *November* 1993)

Abstract—A new mixed model based on the combined mixed functional has been developed for the analysis of problems with bonding conditions and applied to the bimetallic thermostat problem. The mixed formulation has satisfied equilibrium equations, the displacement and the traction boundary conditions, as well as the interfacial continuities of traction in an average sense by virtue of the variational condition of the proposed mixed functional. A mixed finite element (QC 4/8), having no stability problem, has been proposed and successfully applied for the analysis of bonded structures with the selected combination coefficient. A bonding element has been developed based on a patch test-passed quadratic approximation for the relative displacements and bonding tractions in an average sense. Along all the bonding interfaces the results of the mixed method with the continuous stress interpolation were in close agreement with those of the stress formulation based on the principle of complementary virtual work.

1. INTRODUCTION

There has been a continual interest shown in the analysis of thermal stresses at the bonded interfaces of multilayered dissimilar materials subjected to temperature change. A bimetal thermostat has been a controversial problem for the analysis of stresses in thermally mismatched structures, whose first solution, based on the beam theory, was given by Timoshenko (1925). The problem of free edge effects was first addressed by Aleck (1949). More recent solutions include approximate solutions based on strength of materials approach and energy methods (Blech and Kantor, 1984; Suhir, 1986, 1989; Yin, 1991), analytical methods (Kuo, 1989; Lee and Jasiuk, 1991), and finite element methods (Lau, 1989).

Each approach to the thermostat problem has resulted in somewhat different stress behaviors at the interface. For example, the elasticity solutions give singular stresses at the free edge of the interface, while the approximate solutions do not show the singular stresses. Some solutions (Blech and Kantor, 1984; Suhir, 1989; Yin, 1991) satisfy the traction-free condition at the free edge of the interface, but other solutions (Suhir, 1986; Kuo, 1989; Lee and Jasiuk, 1991; Lau, 1989) do not satisfy this condition.

Suhir (1989) presented an approximate method satisfying the zero shear stress condition at the free edge through the modification of his previous method (Suhir, 1986). Lau (1989) pointed out that the interface stresses predicted by the conventional displacement-based finite element (FE) methods are unreliable near the free edge. He suggested a modified FE method, based on the displacement approach with nodal strain calculation, to obtain more accurate solutions near the free edge of the interface. His solutions, however, violated the condition of zero shear at the free edge. Moreover, his method of nodal strain calculation is not commonly available in commercially available packages and, in general, the nodal strains may have more errors than those obtained at Gaussian points.

There are also several attempts to improve the accuracy of stresses along the interface of composite structures (Angelides *et al.*, 1988; Shirazi-Adl, 1989). Recently, Chouchaoui and Shirazi-Adl (1992) proposed a mixed FE formulation based on the Hellinger–Reissner functional for stress analysis of composite structures. They defined as C^1 superelement for each homogeneous region and assembled the superelements into a global matrix. In order

to relax the continuity of stresses at the interface between each homogeneous region, they used a static condensation technique. They applied the method to analyze composite structures without considering the free edge problem.

In the numerical analysis of edge problems the mixed finite element method (FEM) gives better results than the displacement-based FEM, because the latter has many shortcomings in constructing compatible shape functions for C^1 elements, poor performance in constrained media problems, loss of accuracy in calculating derived field variables (including derivatives of primary field variables) and slow convergence for problems with high gradients (Noor, 1983). Since the mixed FEM can overcome some of these shortcomings, it has been used to solve elastic contact problems with high stress gradients and displacement constraints, as shown by Heyliger and Reddy (1987).

Although the mixed model resolved many problems of the single field FE model, it still has difficulties. Since the stiffness matrix of the mixed model is indefinite, the equation solver must be chosen carefully. It is also noted that, due to the violation of the consistency condition, approximation functions might result in spurious mechanisms associated with zero eigenvalues (Oden and Reddy, 1976). Many researchers have tried to overcome these difficulties by proposing new functionals (Slivker, 1982; Felippa, 1989). Recently, Lee and Lee (1990, 1993) proposed a new mixed functional, called the "combined mixed functional", constructed by a linear combination of the Hellinger–Reissner functional and the total potential energy. It has been shown that the bilinear form of the mixed functional is a V-elliptic or a weakly coercive; hence, the variational problem associated with the functional has a unique solution (Lee, 1993). In addition, constraints such as bonding conditions and contact conditions can be successfully incorporated into the functional in terms of Lagrange multipliers. For the independent variables satisfying both the completeness condition and the required continuity, the proposed mixed model generates no spurious zero energy modes, regardless of the approximating polynomials of the independent field variables. Thus, the mixed model enables us to compose the elements with high order approximations, such as linear stress and quadratic displacement.

In this paper, we propose a new mixed FE model based on the combined mixed functional with the bonding condition. The mixed model has been applied for the analysis of general bonding problems including thermal effects. This formulation satisfies equilibrium equations, the displacement and the traction boundary conditions, and the interfacial continuities of traction in an average sense by virtue of the variational condition of the proposed mixed functional. While the displacement-based FE formulation would result in a considerable amount of error along the bonding surface of a composite structure of highly dissimilar materials, this formulation would give reliable solutions along the interface.

A mixed finite element (QC 4/8), having no stability problem, has been developed and successfully used with the selected combination coefficient. A bonding element derived from the bonding condition (i.e. the relative displacements along the interface are zero) not only made the quadratic approximation pass the patch test for the relative displacements and bonding tractions, but also made the normal and shear stress continuous along the interface in an average sense.

The present method has been applied to the bimetallic thermostat problem and the results have been compared with the existing analytical, variational and numerical solutions. Recently, Yin (1991, 1992) developed the variational method using stress functions and the principle of complementary virtual work for the determination of interlaminar thermal stresses in laminated beams. His results indicated that, in the sense appropriate to variational calculus, the stresses for the two-layer bimetal thermostat converged rapidly to an approximate elasticity solution (Kuo, 1989) except near the free edge. Although the variational method (Yin, 1992) and the approximate elasticity methods (Kuo, 1989; Lee and Jasiuk, 1991) are efficient, reliable and powerful tools for attacking these types of problems, they might have some difficulties in solving the problems whose geometry or the displacement boundary conditions, including complex loading conditions, change. In the proposed mixed FEM, such difficulties can be relaxed with the consideration of displacement.

The results of the mixed method with the continuous stress interpolation agreed well with those of the variational solution along the entire bonding interface, but showed some

discrepancies compared with the elasticity solutions near the free edge. For the mixed model with discontinuous stress interpolation and from the displacement FE model, axial and shear stresses near the free edge did not vanish due to inherent limitations of such approaches. Although the elasticity solutions have shown singularity at the free edge, there is no physical significance in this because stress singularity would not occur in real materials. In this sense, the nonlinear material response has to be included in the formulation and the mixed FE formulation including independent stress variables can be considered as promising tools for further research.

2. GOVERNING EQUATION

Figure 1 shows the two-body bonding model considered here. Although the model of Fig. 1 is a two-dimensional problem, the formulation in this paper is developed for three-dimensional elastic problems. In the bonding model, a body 2 is constrained against rigid body motion and the rigid body displacements of a body 1 are described by q_j. Along the boundary Γ of a domain Ω, displacements are specified on Γ_U, and the surface forces are given on Γ_F. The bonding region, Γ_B, is defined as the boundary where no relative motion occurs between two bodies.

Along the bonding boundary, shown in Fig. 2, bonding tractions β_i^k are described as

$$\beta_i^k = \sigma_{ij}^k n_j^k, \tag{1}$$

where n_j^k are the unit normal vectors on the surface of body k. In this paper the superscript k is used to designate a quantity associated with the body k. By convention, repeated subscripts imply summation over the range of them and the notation $(\cdot)_{,j}$ denotes differentiation with respect to a space coordinate x_j. Note that $\beta_i^1 = \beta_i^2 = \beta_i$ along the bonding boundary.

In the body under rigid motion, displacements u_i define relative values apart from the rigid body displacements. Under the assumption of linear elastic material for the deformation process, a set of governing equations of the bonding problem can be described as follows.

1. *Global equilibrium equation of body* 1. The principle of virtual work states the quasi-static equilibrium of body 1 as

$$\int_{\Omega^1} f_i^1 g_{ij}\,dv + \int_{\Gamma_F^1} F_i^1 h_{ij}\,ds = \int_{\Gamma_B} \beta_i \alpha_{ij}\,ds, \tag{2}$$

where F_i^1 and β_i are external forces and bonding tractions exerted on a differential surface

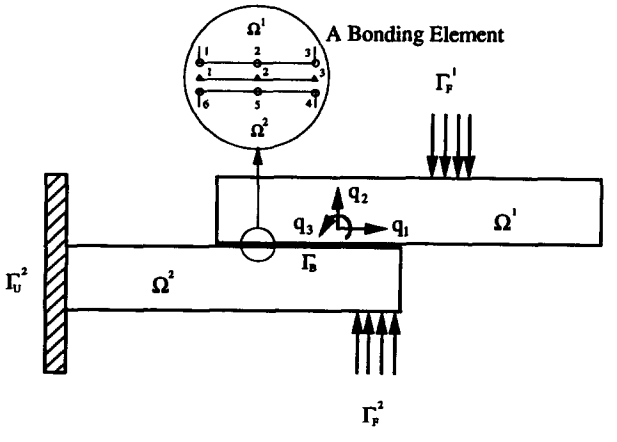

Fig. 1. Schematic model for two-body bonding problems.

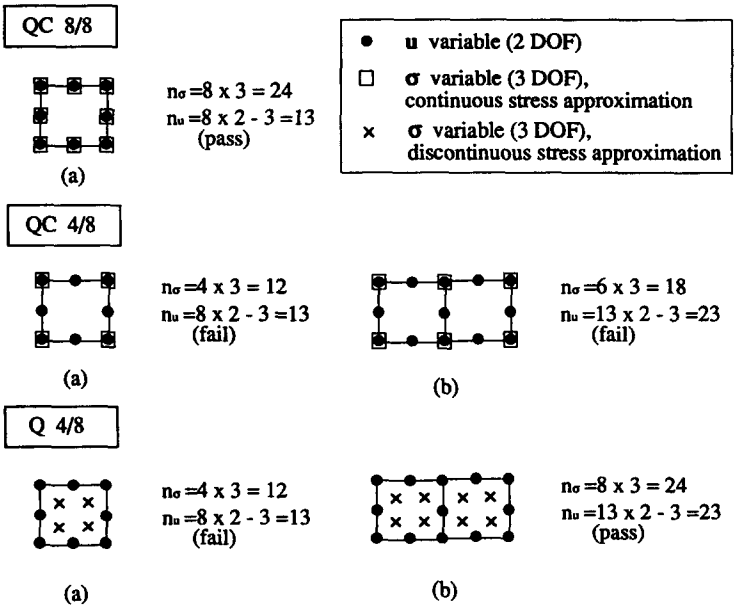

Fig. 2. Patch tests for the mixed σ–**u** formulation with the test condition ($n_\sigma \geqslant n_u$). (a) Single-element patch tests; (b) multiple-element patch tests.

ds, respectively, and f_i^1 is a body force acting on a differential volume dv of body 1. The coefficients h_{ij}, α_{ij} and g_{ij} in eqn (2) represent rigid body displacements on Γ_F^1, on Γ_B and in Ω^1, respectively, where the subscripts ij denote corresponding quantity in the ith coordinate direction due to a unit displacement in the jth rigid body degree of freedom. The coefficients are determined only by kinematic relations for body 1.

2. *Equations of internal equilibrium*

$$\sigma_{ij,j}^k + f_i^k = 0, \tag{3}$$

where f_i^k is the body force in Ω^k.

3. *Strain–displacement relationship*

$$\varepsilon_{ij}^k = \tfrac{1}{2}(u_{i,j}^k + u_{j,i}^k). \tag{4}$$

4. *Stress–strain relationship*

$$\sigma_{ij}^k = a_{ijlm}^k \varepsilon_{lm}^k \tag{5}$$

$$\varepsilon_{ij}^k = A_{ijlm}^k \sigma_{lm}^k, \tag{6}$$

where a_{ijlm}^k is an elasticity tensor in the body k, whose inverse is denoted by A_{ijlm}^k; the repeated superscript k does not mean summation.

5. *Boundary conditions*

$$\sigma_{ij}^k n_j^k = F_i^k, \quad \text{on} \quad \Gamma_F^k \tag{7}$$

$$u_i^k = 0, \quad \text{on} \quad \Gamma_U^k. \tag{8}$$

6. *Compatibility conditions.* The relative motion in the bonded region Γ_B after deformation is described by the following equation

$$g_i = u_i^1 + u_i^2 + \alpha_{ij} q_j. \tag{9}$$

Since no relative motion is allowed on Γ_B, by definition, compatibility conditions between two bodies can be written as

$$g_i = 0 \tag{10}$$

at Γ_B.

The elastic problem under bonding condition is thus summarized by eqns (2)–(8) and (10).

3. COMBINED MIXED FUNCTIONAL

For the mixed formulation proposed in this paper, admissible spaces of **X** and **Y** are defined by independent variables u_i and σ_{ij}, respectively

$$\mathbf{X} = \{\mathbf{u}|\mathbf{u} = \{u_i\}, u_i \in H^1(\Omega), u_i = 0 \text{ on } \Gamma_U\} \tag{11}$$

$$\mathbf{Y} = \{\boldsymbol{\sigma}|\boldsymbol{\sigma} = \{\sigma_{ij}\}, \sigma_{ij} \in H^0(\Omega), \sigma_{ij} = \sigma_{ji}\}, \tag{12}$$

where $H^m(\Omega)$ is the Sobolev space of the mth order.

Although the homogeneous displacement boundary conditions of $u_i = 0$ on Γ_u are assumed in eqn (11), nonhomogeneous displacement boundary conditions can easily be incorporated into the present formulation if some regularity conditions are satisfied for the prescribed displacement fields.

On the product space of **X** and **Y**, the combined mixed functional, J_{CM}, can be defined as (Lee and Lee, 1990)

$$J_{CM} = \frac{\alpha}{2}\int_\Omega A_{ijlm}\sigma_{ij}\sigma_{lm}\,dv - \alpha\int_\Omega \sigma_{ij}\varepsilon_{ij}\,dv + \frac{\alpha+1}{2}\int_\Omega a_{ijlm}\varepsilon_{ij}\varepsilon_{lm}\,dv - \int_\Omega f_i u_i\,dv - \int_{\Gamma_F} F_i u_i\,ds, \tag{13}$$

where α is an arbitrary, nonzero real constant, called the "combination coefficient".

For the thermal problems, the functional can be modified as follows:

$$J_{CM} = \frac{\alpha}{2}\int_\Omega A_{ijlm}\sigma_{ij}\sigma_{lm}\,dv - \alpha\int_\Omega \sigma_{ij}\varepsilon_{ij}\,dv + \alpha\int_\Omega \sigma_{ij}\varepsilon^\theta_{ij}\,dv + \frac{\alpha+1}{2}\int_\Omega a_{ijlm}\varepsilon_{ij}\varepsilon_{lm}\,dv - (1+\alpha)\int_\Omega \varepsilon_{ij}a_{ijlm}\varepsilon^\theta_{lm}\,dv - \int_\Omega f_i u_i\,dv - \int_{\Gamma_F} F_i u_i\,ds, \tag{14}$$

where ε^θ_{ij} is the thermal strain in Ω.

For simplicity in formulation, body forces and thermal effects will be neglected in the following, although they can be easily incorporated. Several approaches are available for treating the compatibility condition of eqn (10); for our bonding element the Lagrange multiplier approach is adopted. The resulting functional, J, is expressed as

$$J = \sum_{k=1}^{2}\left[\frac{\alpha}{2}\int_{\Omega^k} A^k_{ijlm}\sigma^k_{ij}\sigma^k_{lm}\,dv - \alpha\int_{\Omega^k}\sigma^k_{ij}\varepsilon^k_{ij}\,dv + \frac{\alpha+1}{2}\int_{\Omega^k} a^k_{ijlm}\varepsilon^k_{ij}\varepsilon^k_{lm}\,dv - \int_{\Gamma^k_F} F^k_i u^k_i\,ds\right] - \int_{\Gamma^1_F} F^1_i h_{ij} q_j\,ds - \int_{\Gamma_F}\beta_i(u^1_i + u^2_i + \alpha_{ij}q_j)\,ds, \tag{15}$$

where u_i, σ_{ij}, β_i and q_j are independent variables, among which admissible spaces of β_i and q_j are defined as

$$\mathbf{Z} = \{\boldsymbol{\beta}|\boldsymbol{\beta} = \{\beta_i\}, \beta_i \in H^{-1/2}(\Gamma)\} \tag{16}$$

$$\mathbf{W} = \{\mathbf{q}|\mathbf{q} = \{q_i\}, q_i \in H^1(\Omega)\}. \tag{17}$$

The necessary condition of solution is the functional J to be stationary, i.e.

$$\delta J = 0, \tag{18}$$

where the variation of J is taken with respect to u_i, σ_{ij}, β_i and q_j. Taking the first variation of eqn (15) we obtain

$$\delta J = \sum_{k=1}^{2} \left[\alpha \int_{\Omega^k} A^k_{ijlm} \sigma^k_{ij} \delta\sigma^k_{lm} \, dv - \alpha \int_{\Omega^k} \delta\sigma^k_{ij} \varepsilon^k_{ij} \, dv - \alpha \int_{\Omega^k} \sigma^k_{ij} \delta u^k_{i,j} \, dv + (\alpha+1) \right.$$
$$\left. \times \int_{\Omega^k} a^k_{ijlm} \varepsilon^k_{ij} \delta u^k_{i,j} \, dv - \int_{\Gamma^k_F} F^k_i \delta u^k_i \, ds \right] - \int_{\Gamma^1_F} F^1_i h_{ij} \delta q_j \, ds$$
$$- \int_{\Gamma_B} \delta\beta_i (u^1_i + u^2_i + \alpha_{ij} q_j) \, ds - \int_{\Gamma_B} \beta_i (\delta u^1_i + \delta u^2_i + \alpha_{ij} \delta q_j) \, ds. \tag{19}$$

From eqn (19) with eqn (18), the Euler equations, boundary conditions and constraint (or bonding) conditions can be obtained as

$$\sigma^k_{ij,j} = 0, \quad \text{in} \quad \Omega^k \tag{20}$$

$$\varepsilon^k_{ij} = A^k_{ijlm} \sigma^k_{lm}, \quad \text{in} \quad \Omega^k \tag{21}$$

$$\sigma^k_{ij} n^k_j = F^k_i, \quad \text{on} \quad \Gamma^k_F \tag{22}$$

$$\sigma^k_{ij} n^k_j = \beta_i, \quad \text{on} \quad \Gamma_B \tag{23}$$

$$u^1_i + u^2_i + \alpha_{ij} q_j = 0, \quad \text{on} \quad \Gamma_B \tag{24}$$

$$\int_{\Gamma^1_F} F^1_i h_{ij} \, ds = \int_{\Gamma_B} \beta_i \alpha_{ij} \, ds, \quad \text{for body 1.} \tag{25}$$

In eqns (23) and (24), it is observed that the Lagrange multipliers β_i represent bonding tractions, recovering the bonding condition. Hence the functional J is suitable for the bonding problem.

4. FINITE ELEMENT APPROXIMATION

We will consider the domain discretized into element domains Ω_e

$$\bar{\Omega} = \bigcup_{e=1}^{n_E} \bar{\Omega}_e$$
$$\Omega_i \cap \Omega_j = \varnothing, \quad \text{if} \quad i \neq j, \tag{26}$$

where subscripts e are element numbers, and $\bar{\Omega}$ means a closure of the set, i.e. a union of the set with its boundary. The boundary Γ_e of a finite element Ω_e is assumed to be continuous in the sense of Lipschitz.

Linear spaces $\mathbf{X}^h$, $\mathbf{Y}^h$, $\mathbf{Z}^h$ and $\mathbf{W}^h$ are finite dimensional subspaces of admissible displacements, stresses, bonding tractions and rigid body displacements, respectively defined in eqns (11), (12), (16) and (17). By imposing the stationary condition on the functional J of eqn (15) with respect to the independent variables (displacements, stresses, bonding tractions and rigid body displacements) we can obtain the weak forms as follows:

$$(1+\alpha)\int_{\Omega_e^k} a_{ijlm}^k e_{ij}^k \varepsilon_{lm}^k \,\mathrm{d}v - \alpha\int_{\Omega_e^k} e_{ij}^k \sigma_{ij}^k \,\mathrm{d}v - \int_{\Gamma_{eF}^k} v_i^k \beta_i \,\mathrm{d}s = \int_{\Gamma_{eF}^k} F_i^k v_i^k \,\mathrm{d}s, \quad \forall v_i \in \mathbf{X}^h$$

$$\alpha\int_{\Omega_e^k} A_{ijlm}^k s_{ij}^k \sigma_{lm}^k \,\mathrm{d}v - \alpha\int_{\Omega_e^k} s_{ij}^k \varepsilon_{ij}^k \,\mathrm{d}v = 0, \quad \forall s_{ij} \in \mathbf{Y}^h$$

$$\int_{\Gamma eB} b_i(u_i^1 + u_i^2 + \alpha_{ij} q_j) \,\mathrm{d}s = 0, \quad \forall b_i \in \mathbf{Z}^h$$

$$\int_{\Gamma_{eF}^1} F_i^1 h_{ij} r_j \,\mathrm{d}s + \int_{\Gamma_{eB}} \beta_i \alpha_{ij} r_j \,\mathrm{d}s = 0, \quad \forall r_i \in \mathbf{W}^h, \tag{27}$$

where v_i^k, s_{ij}^k, b_i and r_i are admissible variations of u_i^k, σ_{ij}^k, β_i and q_i, respectively, and forces and boundary conditions are described on the boundaries Γ_{eF}^k and Γ_{eB}^k. The tensor $e^k = \{e_{ij}^k\}$ is the virtual strain obtained from the virtual displacement vector.

For the finite elements formulated in eqn (27), each of the unknowns is approximated by an appropriate shape function with unknown parameters. The displacement $u_i \in \mathbf{X}^h$, having n_u^e degrees of freedom in an element, is approximated by

$$\mathbf{u} = \mathbf{N}_u^e \bar{\mathbf{u}}^e, \tag{28}$$

where $\bar{\mathbf{u}}^e$ represents the nodal parameters to be determined and $\mathbf{N}_u^e$ the appropriate shape function. On this basis, the strain vector $\boldsymbol{\varepsilon}$ can be approximated in terms of the displacement field $\bar{\mathbf{u}}^e$

$$\varepsilon = \mathbf{B}\bar{\mathbf{u}}^e, \tag{29}$$

where $\mathbf{B}$ is the matrix derived from eqn (4).

The stresses $\sigma_{ij} \in \mathbf{Y}^h$, having n_σ^e degrees of freedom per element, are approximated as

$$\sigma = \mathbf{N}_\sigma^e \bar{\sigma}^e, \tag{30}$$

where $\bar{\sigma}^e$ denotes unknown coefficient vector and $\mathbf{N}_\sigma^e$ stands for assumed stress shape function matrix.

On the bonding boundary of an element, the bonding traction $\beta_i \in \mathbf{Z}^h$, having n_β^e degrees of freedom per element, can be interpolated as

$$\beta = \mathbf{N}_\beta^e \bar{\beta}^e, \tag{31}$$

where $\bar{\beta}^e$ is the unknown coefficient vector and $\mathbf{N}_\beta^e$ denotes the assumed shape function of the bonding traction.

The rigid body displacements, $q_i \in \mathbf{W}^h$, of n_q degrees of freedom, can be given as

$$\mathbf{q} = \bar{\mathbf{q}}^e. \tag{32}$$

The substitution of eqns (28)–(32) into eqn (27) results in the following mixed finite element equations

$$\begin{bmatrix} (1+\alpha)\mathbf{K}^e & -\alpha\mathbf{G}^e & \mathbf{L}^e & \mathbf{0} \\ -\alpha\mathbf{G}^{eT} & \alpha\mathbf{M}^e & \mathbf{0} & \mathbf{0} \\ \mathbf{L}^{eT} & \mathbf{0} & \mathbf{0} & \mathbf{Q}^e \\ \mathbf{0} & \mathbf{0} & \mathbf{Q}^{eT} & \mathbf{0} \end{bmatrix} \begin{Bmatrix} \bar{\mathbf{u}}^e \\ \bar{\sigma}^e \\ \bar{\beta}^e \\ \bar{\mathbf{q}}^e \end{Bmatrix} = \begin{Bmatrix} \bar{\mathbf{F}}_u^e \\ \mathbf{0} \\ \mathbf{0} \\ \bar{\mathbf{F}}_q^e \end{Bmatrix}, \tag{33}$$

where

$$\mathbf{K}^e = \int_{\Omega^e} \mathbf{B}^T\mathbf{D}\mathbf{B}\,dv$$

$$\mathbf{G}^e = \int_{\Omega^e} \mathbf{B}^T\mathbf{N}_\sigma\,dv$$

$$\mathbf{M}^e = \int_{\Omega^e} \mathbf{N}_\sigma^T\mathbf{D}^{-1}\mathbf{N}_\sigma\,dv$$

$$\mathbf{L}^e = -\int_{\Gamma_B^e} \mathbf{N}_u^T\mathbf{T}_\beta\mathbf{N}_\beta\,ds$$

$$\mathbf{Q}^e = -\int_{\Gamma_B^e} \mathbf{N}_\beta^T\mathbf{T}_\beta\mathbf{A}\,ds$$

$$\bar{\mathbf{F}}_u^e = \int_{\Gamma_F^e} \mathbf{N}_u^T\mathbf{F}\,ds$$

$$\bar{\mathbf{F}}_q^e = \int_{\Gamma_F^e} \mathbf{H}\mathbf{F}\,ds, \tag{34}$$

where $\mathbf{D}$ denotes the matrix form of the elasticity tensor; $\mathbf{D}^{-1}$, the inverse of $\mathbf{D}$; $\mathbf{A}$ and $\mathbf{H}$, the kinematic relation matrices corresponding to α_{ij}, h_{ij} in eqn (2), respectively; $\mathbf{T}_\beta$, the transformation matrix provides us with a convenience of numerical integration through the conversion of the rectangular coordinate components of bonding traction into the normal and tangential coordinate components.

In the formulation given above the displacement fields should be C^0 continuous, but stresses and tractions are allowed to be discontinuous at element interfaces. Therefore, the stresses can be approximated by continuous or discontinuous interpolation. If the stress field is approximated by globally C^0 continuous functions, the global equivalent displacement stiffness matrix $\bar{\mathbf{K}}$ becomes a symmetric full matrix. In that case we have to cope with the immense matrix size at the expense of obtaining more accurate results for the stresses.

We can eliminate $\bar{\sigma}^e$ at the element level in case of discontinuous stress approximation

$$\begin{bmatrix} \bar{\mathbf{K}}^e & \mathbf{L}^e & \mathbf{0} \\ \mathbf{L}^{eT} & \mathbf{0} & \mathbf{Q}^e \\ \mathbf{0} & \mathbf{Q}^{eT} & \mathbf{0} \end{bmatrix} \begin{Bmatrix} \bar{\mathbf{u}}^e \\ \bar{\beta}^e \\ \bar{\mathbf{q}}^e \end{Bmatrix} = \begin{Bmatrix} \bar{\mathbf{F}}_u^e \\ \mathbf{0} \\ \bar{\mathbf{F}}_q^e \end{Bmatrix}, \tag{35}$$

where $\bar{\mathbf{K}}^e = (1+\alpha)\mathbf{K}^e - \alpha\mathbf{G}^e\mathbf{M}^{e-1}\mathbf{G}^{eT}$ which is called an equivalent displacement stiffness matrix.

Eliminating $\bar{\mathbf{u}}^e$ in eqn (35), we have

$$\begin{bmatrix} \mathbf{B}^e & \mathbf{Q}^e \\ \mathbf{Q}^{eT} & \mathbf{0} \end{bmatrix} \begin{Bmatrix} \bar{\beta}^e \\ \bar{\mathbf{q}}^e \end{Bmatrix} = \begin{Bmatrix} \bar{\mathbf{F}}_\beta^e \\ \bar{\mathbf{F}}_q^e \end{Bmatrix}, \tag{36}$$

where $\mathbf{B}^e = -\mathbf{L}^{eT}\bar{\mathbf{K}}^{e-1}\mathbf{L}^e$ and $\bar{\mathbf{F}}_\beta^e = -\mathbf{L}^{eT}\bar{\mathbf{K}}^{e-1}\bar{\mathbf{F}}_u^e$. If there exists rigid body motion in the system, we can eliminate $\bar{\beta}^e$ using the first equation of eqn (36), obtaining the following equation with only one independent variable

$$-\mathbf{Q}^{eT}\mathbf{B}^{e-1}\mathbf{Q}^e\bar{\mathbf{q}}^e = \bar{\mathbf{F}}_q^e - \mathbf{Q}^{eT}\mathbf{B}^{e-1}\bar{\mathbf{F}}_\beta^e. \tag{37}$$

Based on the element equations of eqn (37), we can easily obtain the global system equations by applying the usual assembling procedure.

5. SELECTION OF APPROXIMATION FUNCTIONS

After the conventional assembling procedure, eqn (35) can be decomposed as follows:

$$\begin{bmatrix} \bar{\mathbf{K}}_{AA} & \bar{\mathbf{K}}_{AB} & \mathbf{0} & \mathbf{0} \\ \bar{\mathbf{K}}_{BA} & \bar{\mathbf{K}}_{BB} & \mathbf{L} & \mathbf{0} \\ \mathbf{0} & \mathbf{L}^T & \mathbf{0} & \mathbf{Q} \\ \mathbf{0} & \mathbf{0} & \mathbf{Q}^T & \mathbf{0} \end{bmatrix} \begin{Bmatrix} \bar{\mathbf{u}}_A \\ \bar{\mathbf{u}}_B \\ \bar{\beta} \\ \bar{\mathbf{q}} \end{Bmatrix} = \begin{Bmatrix} \bar{\mathbf{F}}_A \\ \bar{\mathbf{F}}_B \\ \mathbf{0} \\ \bar{\mathbf{F}}_q \end{Bmatrix}. \tag{38}$$

Here, the global displacement vector $\bar{\mathbf{u}}$ is decomposed into the nodal displacement vector $\bar{\mathbf{u}}_B$ in the bonding zone and the $\bar{\mathbf{u}}_A$ in remaining part. A corresponding partition also holds for the equivalent displacement stiffness matrix $\bar{\mathbf{K}}$. On the elimination of $\bar{\mathbf{u}}_A$ using the first row of eqn (38), we have

$$\begin{bmatrix} \hat{\mathbf{K}}_{BB} & \mathbf{L} & \mathbf{0} \\ \mathbf{L}^T & \mathbf{0} & \mathbf{Q} \\ \mathbf{0} & \mathbf{Q}^T & \mathbf{0} \end{bmatrix} \begin{Bmatrix} \bar{\mathbf{u}}_B \\ \bar{\beta} \\ \bar{\mathbf{q}} \end{Bmatrix} = \begin{Bmatrix} \hat{\mathbf{F}}_B \\ \mathbf{0} \\ \bar{\mathbf{F}}_q \end{Bmatrix}, \tag{39}$$

where $\hat{\mathbf{K}}_{BB} = \bar{\mathbf{K}}_{BB} - \bar{\mathbf{K}}_{BA}\bar{\mathbf{K}}_{AA}^{-1}\bar{\mathbf{K}}_{AB}$ and $\hat{\mathbf{F}}_B = \bar{\mathbf{F}}_B - \bar{\mathbf{K}}_{BA}\bar{\mathbf{K}}_{AA}^{-1}\bar{\mathbf{F}}_A$.

Equation (39) is a typical form of mixed approximation. In order that the mixed model corresponding to eqn (39) would satisfy the stability condition, the following conditions should be satisfied for isolated patches (Zienkiewicz and Taylor, 1989)

$$n_d + n_q \geqslant n_b, \qquad n_b \geqslant n_q, \tag{40}$$

where n_d and n_b designate the degrees of freedom in relative displacements and those in bonding tractions, respectively, and n_q denotes the number of degrees of freedom in rigid body displacements for the body including rigid body motion.

Although the present formulation is developed for three-dimensional elastic problems, numerical experiments will be made only on two-dimensional problems for the sake of convenience.

Figure 1 shows a two-dimensional plane stress bonding element which has a quadratic approximation for both of the relative displacements and the bonding tractions along the interface, i.e. $n_d = 6$, $n_b = 6$. Since rigid body modes are fewer than three in the two-dimensional problem, the stability conditions are satisfied under the quadratic approximations of relative displacements and bonding tractions. Therefore, the order of approximation is proper for the numerical analysis of the bonding problems.

Without bonding boundary, the eqn (35) can be reduced to the following

$$\begin{bmatrix} (1+\alpha)\mathbf{K}^e & -\alpha\mathbf{G}^e \\ -\alpha\mathbf{G}^{eT} & \alpha\mathbf{M}^e \end{bmatrix} \begin{Bmatrix} \bar{\mathbf{u}}^e \\ \bar{\sigma}^e \end{Bmatrix} = \begin{Bmatrix} \bar{\mathbf{F}}_u^e \\ \mathbf{0} \end{Bmatrix}. \tag{41}$$

The property of the system matrix of eqn (41) is dependent on the combination coefficient, α. In the case of $\alpha = -1$, eqn (41) becomes a matrix equation based on the Hellinger–Reissner functional, while in the case of $\alpha = 0$, it becomes a matrix equation based on the total potential energy functional.

In order to obtain improved solutions in energy sense, it is desirable to take $-1 < \alpha < 0$. In this range of α, Felippa (1989) proved that the combined mixed functional is smaller than the total potential energy functional. For $-1 < \alpha < 0$, Lee (1993) proved that the bilinear form of the combined mixed functional is weakly coercive and that the functional has a unique solution.

Note that, for the mixed models based on the Hellinger–Reissner variational principle, the stability conditions should be imposed on the order of approximating polynomials, since a violation of the conditions may lead to non-unique solutions. In the present formulation, however, the stresses can be approximated safely without any consideration of displacement

approximation, since corresponding bilinear forms are weakly coercive as far as stresses are $\mathbf{H}^0(\Omega)$ functions.

Figure 2 shows a two-dimensional plane stress problem and several elements, in which $\mathbf{N}_\sigma^e$ can be continuous or discontinuous between elements while $\mathbf{N}_u^e$ has to be continuous. The quadrilateral mixed element with continuous stress approximation is denoted by QC n/m, where n and m are the numbers of nodes used for stress approximation and for displacement approximation, respectively. In the mixed elements based on the Hellinger–Reissner theory, we find that the QC 4/8 fails both the multiple-element patch test and the single-element patch test for the mixed elements (Zienkiewicz and Taylor, 1989), while the QC 8/8 passes the tests. The QC 4/8, which fails in the single-element patch test, passes the patch test for assemblies of two or more elements. However, it is possible to construct both the QC 4/8 and the QC 8/8 from the combined mixed functional without the stability problem. In these elements, discontinuous stress approximation can be easily obtained through the elimination of stress vector at an element level.

The accuracy of the elements varies with the combination coefficient, α. It is pointed out that, in the range of combination coefficients of $-1 < \alpha < 0$, the combined mixed functional results in smaller energy than the potential energy and has a unique solution. However, it is still an open problem of which value of α induces the more accurate solutions in numerical experiments.

For the cantilever beam bending problem of Fig. 3, we investigate the numerical behavior of solutions associated with element distortion, e. For the QC 4/8 and the QC 8/8, we investigate variations in the x-directional stress at point D and the y-directional displacement at point A.

Figures 4 and 5 compare exact and numerical solutions for the y-directional displacement at point A and those for the axial stress at point D in the combination coefficient range of -3 to 3. The combination coefficients seem to have little effect on the accuracy of the solutions for moderately distorted mesh. For the more distorted mesh, however, the effect becomes more severe according to the value of combination coefficient. For the coefficient, α, greater than -1, the behaviors of both elements are almost identical. As the coefficient, α, approaches -1, the solutions of both elements converge closely to exact solutions.

The displacement solutions of the QC 4/8 rapidly converge as the coefficient, α, is close to -1 while those of the QC 8/8 converge slowly. For stresses the QC 8/8 gives accurate solutions regardless of the coefficient, α, and of the mesh distortion, e, while the solutions of the QC 4/8 are closely related with the coefficient but converge rapidly. If the coefficient is smaller than -1, the stress solutions of the QC 4/8 converge to exact solutions as α approaches -1, while those of the QC 8/8 for $e = 2$ diverge. We note that the number of stress degrees of freedom in the QC 4/8 is a half of that in the QC 8/8, but the QC 4/8

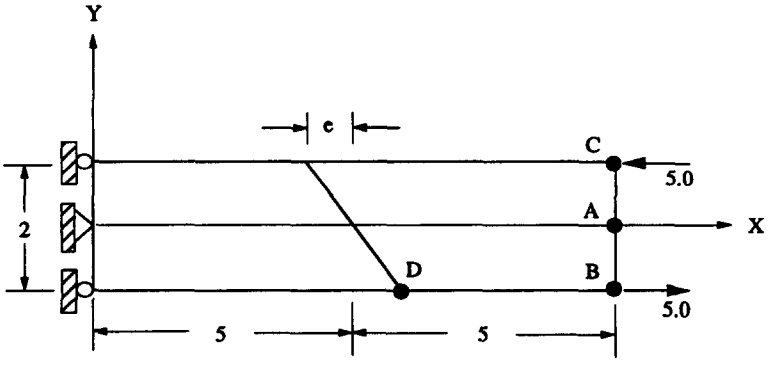

E = 1000 , v = 0.3

Fig. 3. A model to compare effect of element distortion and variation of combination coefficient for each method.

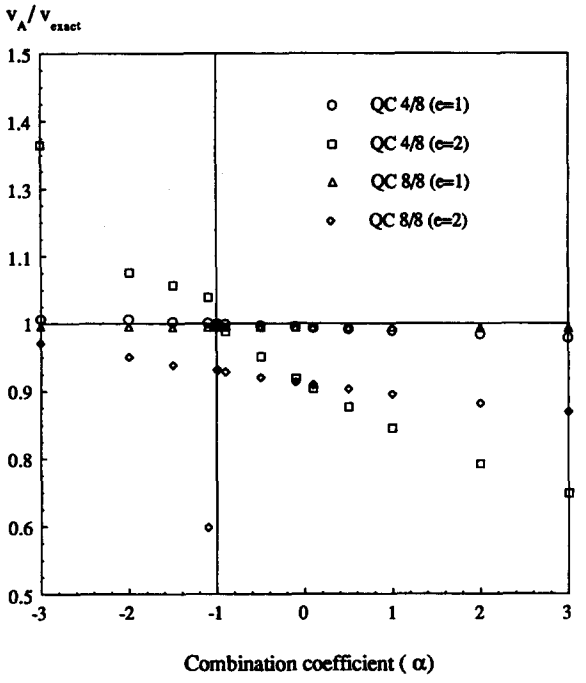

Fig. 4. Displacement deviation (at point A) due to the variation of combination coefficient.

with a proper combination coefficient is superior to the QC 8/8. It is also noted that the selection of the combination coefficient might affect only the convergence rate of the mixed elements.

In this study, we have chosen the QC 4/8 with $\alpha = -0.999$ considering that α should be greater than -1, as close as possible to -1 and large enough to be distinguished from the round-off error. However, further investigation is required to determine the best approximation schemes with the most desirable coefficient. It is also noted that the combined mixed functional can be closely related with the stabilization method (Lee and Lee, 1993),

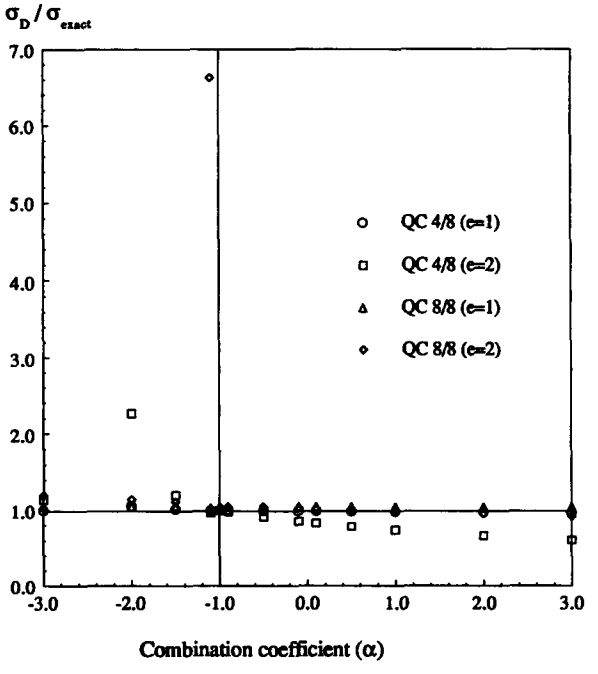

Fig. 5. Stress deviation (at point D) due to the variation of combination coefficient.

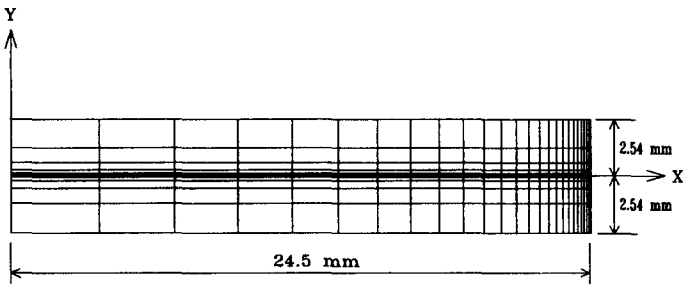

Fig. 6. Finite element models for a half of the bimetallic thermostat (mesh 3).

where the stabilization coefficient has been set to be a small positive number, typically, 0.001 (corresponding to $\alpha = -0.999$) through a number of numerical experiments.

6. NUMERICAL EXAMPLES AND DISCUSSIONS: ANALYSIS OF A BIMETALLIC THERMOSTAT

Figure 6 shows the FE model (mesh 3) of a bimetallic thermostat, composed of two material layers of molybdenum (upper) and aluminum (lower). Due to symmetry, only a half of the composite structure is considered. The geometrical and material data of the thermostat are given as follows:

$$h_1 = 2.54 \text{ mm}, \quad E_1 = 325 \text{ GPa}, \quad \nu_1 = 0.293, \quad \alpha_1 = 4.9 \times 10^{-6}/^\circ\text{C},$$
$$h_2 = 2.54 \text{ mm}, \quad E_2 = 70.38 \text{ GPa}, \quad \nu_2 = 0.345, \quad \alpha_2 = 23.6 \times 10^{-6}/^\circ\text{C}.$$

Finite element models are constructed by 250 two-dimensional plane stress elements; 125 elements per layer of the thermostat. The element QC 4/8 is used for the mixed model and the CPS8 of ABAQUS (1992) for the displacement-based model. The nodal displacements are fixed in the x-direction along the center line.

The bimetallic thermostat is uniformly heated from the ambient temperature so that ΔT would be 240°C. In order to show free edge effects, the density of element mesh in stress concentration areas (right interface edge) is increased from mesh 1 to mesh 3, where the bias along the x-axis is 1.0, 1.111 and 1.827, respectively, and along the y-axis is 1.0, 0.7, 0.5, respectively.

Figures 7–10 show the axial and interlaminar stress solutions normalized by $E_1\alpha_1\Delta T$ (=382.2 MPa). The solutions obtained from the proposed mixed method are compared

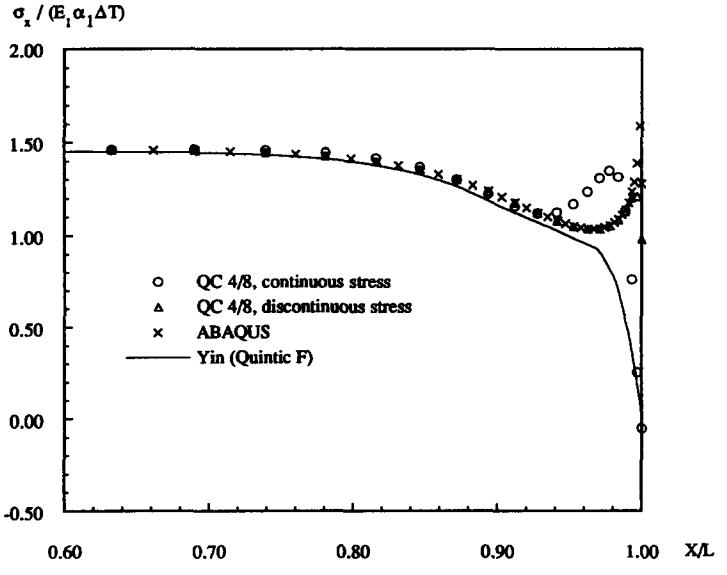

Fig. 7. Normalized axial stresses for mesh 3 along the interface on the upper layer.

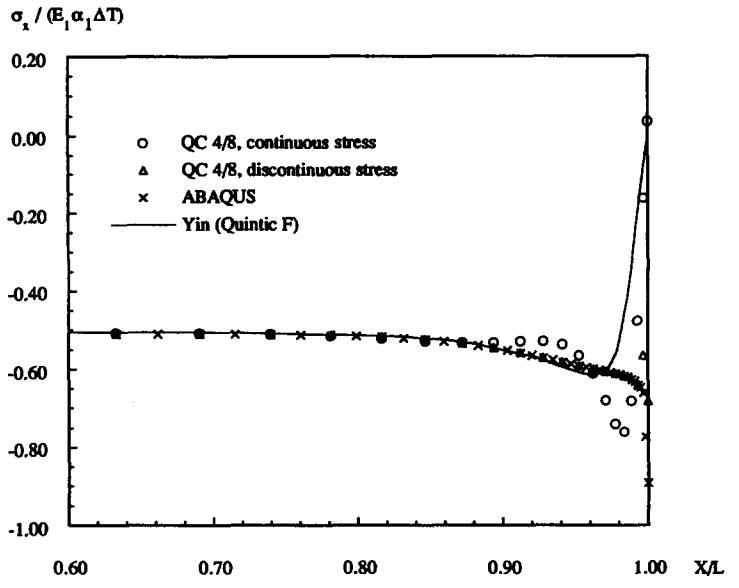

Fig. 8. Normalized axial stresses for mesh 3 along the interface on the lower layer.

with those from the displacement-based FE solution (ABAQUS, 1992) and the variational solution (Yin, 1992). The stresses from the displacement-based FEM are obtained by the option (POSITION = AVERAGED AT NODES) of ABAQUS for two domains. The axial stresses (each domain) are plotted at bonded interface. The interlaminar stresses are averaged at the interface. The results of Yin (1992) are plotted only when the stress function's order is quintic.

Figures 7 and 8 show the axial stresses for mesh 3 on the upper and lower sides of the thermostat interface, respectively. The results of the mixed method with the continuous stress interpolation are in close agreement with those of the variational solution (Yin, 1992). In Suhir's (1986) solution and Yin's (1992) solution, the axial stress is enforced to vanish at the free edge by imposing the boundary condition of vanishing traction. In the mixed solution with continuous stress interpolation, however, the stresses nearly vanish at the free edge without imposing the boundary condition. The stresses of the mixed method based on the discontinuous stress interpolation and the displacement-based FE method (ABAQUS)

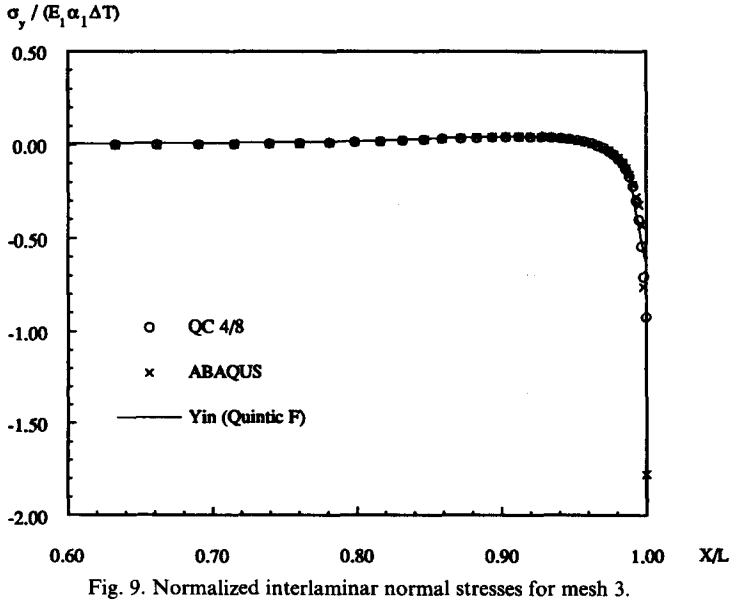

Fig. 9. Normalized interlaminar normal stresses for mesh 3.

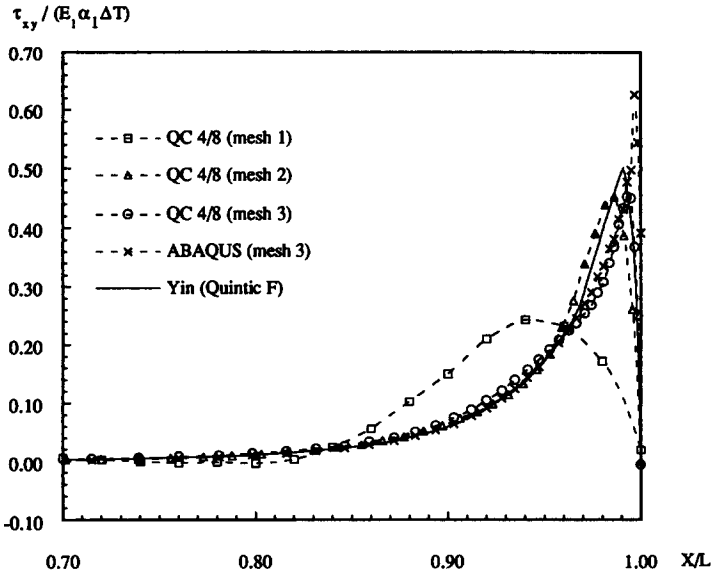

Fig. 10. Normalized interlaminar shear stresses for different mesh types.

do not vanish at the free edge, but they match very well with the mixed solution based on the continuous stress interpolation except near the free edge. It is noted that the mixed solution with continuous stress interpolation and the variational solution show significant discrepancies with the elasticity solution which has unbounded values of σ_x at the free edge (Kuo, 1989; Lee and Jasiuk, 1991). Except extremely near the free edge, however, these solutions are generally in close agreement with those of the elasticity solutions.

Figures 9 and 10 show the results for the interlaminar normal and shear stresses in the vicinity of the free edge. Figure 9 shows the interlaminar normal stress σ_y. Except in an extremely small region adjacent to the free edge, the three results are all in close agreement. In Fig. 10, the interlaminar shear stress based on mixed method with continuous stress interpolation decreases to zero as with the variational solution, but the shear stress based on the displacement-based FE method does not decrease sufficiently at the free edge. Better convergencies are observed for a finer mesh near the free edge. The peak value of the shear stress increases with the refinement of the finite element and the position of the peak value moves toward the free edge. This tendency was also pointed out for the variational solution (Yin, 1992), where the peak value of the interlamina shear stress τ_{xy} increased with the order of the polynomials for the stress function.

From this point of view, the mixed interlaminar shear stress shows significant discrepancies with the elasticity solutions (Kuo, 1989; Lee and Jasiuk, 1991) in an immediate neighborhood of the free edge. Outside this neighborhood, the mixed solutions converge rapidly to the elasticity solutions. The elasticity solutions are singular as expected by theory of elasticity. In reality, however, the material does not sustain infinite stresses, but the material shows the nonlinear material response including the effect of plasticity. Therefore, for a realistic analysis, the nonlinear material behavior has to be included in a formulation. In that sense, the mixed formulation including independent stress variables can be one of the potential tools to accommodate the material plasticity. The maximum displacement from the mixed model (at $X/L = 1.0$, mesh 3) was obtained as 0.364 mm. This is in excellent agreement with the closed-form solution, 0.366 mm, given by Suhir (1986).

The results from the mixed method with continuous stress interpolation behave similarly to those from the variational method (Yin, 1992), since both methods are based on the energy functional. In this point of view, the displacement-based FE solution and the mixed solution with discontinuous stress interpolation have to converge to the variational solution even in the region adjacent to the free edge. However, the solutions showed some discrepancy with the variational solution. Since two solutions are based on the single field functional (only displacement) for each domain, they have such shortcomings as loss of

accuracy in calculating derived field variables and slow convergence for problems with high gradients (Noor, 1983). This tendency is shown at the one or two elements adjacent to the free edge. Although the displacement-based FE method gives reasonable solutions in this problem, the method might induce a considerable amount of error along the bonding surface of highly dissimilar materials, because inter-element continuity cannot be enforced in terms of stresses but displacements alone (Shirazi-Adl, 1989).

Analytic methods are one of several attractive tools for solving the elastic problems. They give a lot of information and physical meaning to understand the problems. The variational methods are efficient and reliable for the analysis of two-layer beams with or without a thin adhesive layer. On the other hand, these methods will result in some difficulties for the complex loading condition problems whose model's geometry or displacement boundary condition are changed. Since the proposed mixed method has no such problems, the method may result in many applications including those in electronic packaging problems.

7. CONCLUSION

A new mixed model based on the combined mixed functional with the bonding condition has been developed for the analysis of general bonding problems and programmed for the two-dimensional bonding problems including thermal effect in this paper. The new mixed model has satisfied equilibrium equations, the displacement and the traction boundary conditions, as well as the interfacial continuities of traction in an average sense by virtue of the variational condition of the proposed mixed functional. Contrary to the displacement-based FE formulation which may induce a considerable amount of error along the bonding surface of a composite structure composed of highly dissimilar materials, the mixed functional formulation always gives reliable solutions along the interface.

A mixed finite element (QC 4/8), having no stability problem, has been proposed and successfully used with the selected combination coefficient for analysis of structures. A bonding element, derived from the bonding condition, passed the patch test with quadratic approximation of both the relative displacements and bonding tractions and the element enforced the normal and shear stress continuity along the interface in an average sense.

The present method has been applied to the bimetallic thermostat problem and the results are compared with the existing elasticity, variational and numerical solutions. The results of the mixed method with the continuous stress interpolation were in close agreement with those of the variational solution along the all bonding interface, but showed some discrepancies to the elasticity solutions near the free edge. Better convergency was observed for finer mesh near the free edge.

Acknowledgement—The authors would like to thank Dr Young-Ho Cho of the Mechanical Engineering Research Institute of the KAIST for his constructive suggestions and strong support.

REFERENCES

ABAQUS (1992). A finite element analysis program. Hibbit, Karlsson & Sorensen, Inc.

Aleck, B. J. (1949). Thermal stresses in a rectangular plate clamped along the edge. *J. appl. Mech.* **16,** 118–122.

Angelides, M., Shirazi-Adl, A., Shrivastava, S. C. and Ahmed, A. M. (1988). A stress compatible finite element for implant/cement interface analysis. *J. Biomech. Engng* **110,** 43–49.

Blech, J. J. and Kantor, Y. (1984). An edge problem having no singularity at the corner. *Comput. Struct.* **18,** 609–617.

Chouchaoui, B. and Shirazi-Adl, A. (1992). A mixed finite element formulation for the stress analysis of composite structures. *Comput. Struct.* **43,** 687–698.

Felippa, C. A. (1989). The extended free formulation of finite elements in linear elasticity. *J. appl. Mech.* **56,** 609–615.

Heyliger, P. R. and Reddy, J. N. (1987). A mixed computational algorithm for plane elastic contact problems. *Comput. Struct.* **26,** 621–653.

Kuo, A. Y. (1989). Thermal stresses at the edge of a bimetallic thermostat. *J. appl. Mech.* **56,** 585–589.

Lau, J. H. (1989). A note on the calculation of thermal stresses in electronic packaging by finite element methods. *J. Electronic Packaging* **111,** 313–320.

Lee, M. and Jasiuk, I. (1991). Asymptotic expansions for the thermal stresses in bonded semi-infinite bimaterial strips. *J. Electronic Packaging* **113,** 173–177.

Lee, Y. J. (1993). Mathematical and numerical analysis of the Mindlin plate element using the stabilization method. Mech. Engng Ph.D. thesis, Korea Advanced Institute of Science and Technology, Taejon.

Lee, Y. J. and Lee, B. C. (1990). A new mixed functional proposed for the analysis of linear elastic problems. *Comput. Struct.* **37,** 1031–1035.

Lee, Y. J. and Lee, B. C. (1993). Derivation of stabilization matrices for Mindlin plates from the combined mixed functional and their mathematical characteristics. *Comput. Struct.* **46,** 21–32.

Noor, A. K. (1983). Multifield (mixed and hybrid) finite element methods. In *State-of-the-art Survey on Finite Element Technology* (Edited by A. K. Noor and W. D. Pilkey), pp. 127–162. ASME, New York.

Oden, J. T. and Reddy, J. N. (1976). On mixed finite element approximations. *SIAM J. Numer. Anal.* **13,** 393–404.

Shirazi-Adl, A. (1989). An interface continuous stress penalty formulation for the finite element analysis of composite media. *Comput. Struct.* **33,** 951–956.

Slivker, V. I. (1982). Mixed variational formulation of problems for elastic systems. *Mechanics of Solids* **17,** 88–97.

Suhir, E. (1986). Stresses in bi-metal thermostats. *J. appl. Mech.* **53,** 657–660.

Suhir, E. (1989). Interfacial stresses in bimetal thermostats. *J. appl. Mech.* **56,** 595–599.

Timoshenko, S. (1925). Analysis of bi-metal thermostats. *J. Optical Soc. Am.* **11,** 233–255.

Yin, W. L. (1991). Thermal stresses and free-edge effects in laminated beams: a variational approach using stress functions. *J. Electronic Packaging* **113,** 68–75.

Yin, W. L. (1992). Refined variational solutions of the interfacial thermal stresses in a laminated beam. *J. Electronic Packaging* **114,** 193–198.

Zienkiewicz, O. C. and Taylor, R. L. (1989). *The Finite Element Method*, 4th Edn, Vol. 1. McGraw-Hill, London.